

# Seismic performance and design of bridge piers with rocking isolation

Xingchong Chen, Xiushen Xia\*, Xiyin Zhang and Jianqiang Gao

School of Civil Engineering, Lanzhou Jiaotong University, Lanzhou 730070, China

(Received March 4, 2019, Revised September 2, 2019, Accepted October 15, 2019)

**Abstract.** Seismic isolation technology has a wide application to protect bridges from earthquake damage, a new designed bridge pier with seismic isolation are provided for railways in seismic regions of China. The pier with rocking isolation is a self-centering system under small and moderate earthquakes, and the unbonded prestressed tendons are used to prevent overturning under strong earthquakes. A numerical model based on pseudo-static testing results is presented to evaluate the seismic performance of isolation bridge piers, and is validated by the shaking table test. It is found that the rocking response and the loss of prestressing for the bridge pier increase with the increase of earthquake intensity. Besides, the intensity and spectral characteristics of input ground motion have great influence on displacement of the top and bottom of the bridge pier, while have less influence on the bending moment of the pier bottom. Experimental and numerical results show that the rocking-isolated piers presented in this study have good seismic performance, and it provides an alternative way for the railway bridge in the regions with high occurrence of earthquakes. Therefore, we provide the detailed procedures for seismic design of the rocking-isolated bridge pier, and a case study of the seismic isolation design with rocking piers is carried out to popularize the seismic isolation methods.

**Keywords:** railway bridges; seismic isolation with rocking pier; prestressed tendon; shaking table test; numerical simulation; seismic performance and design

## 1. Introduction

Severe earthquakes are random events that may have a devastating outcome for structures and lifelines (Fragiadakis, Vamvatsikos *et al.* 2015). Serious damage could occur on bridge structures during major earthquakes, especially for bridge piers (Chung, Park *et al.* 2006; Li, Guan *et al.* 2014). There are several measures to reduce seismic vibration of bridge piers, including viscous damper (VD), triple friction pendulum (TFP) system (Shao, Ju *et al.* 2017), lead rubber bearings (LRBs) (Ozdemir, Bayhan *et al.* 2018), and tuned mass damper (TMD) (Chen, Han *et al.* 2018) or a hybrid seismic response control (HSRC) system (Heo, Kim *et al.* 2017). While, most of railway bridge piers constructed in seismic regions of China are featured with large size (Chen, Ding *et al.* 2018; Ding, Chen *et al.* 2018), the inertia force induced by the self-weight of the railway bridge pier cannot be neglected during earthquakes. It is clear that base-isolation bearings can protect the bridge substructure by restricting the transmission of horizontal acceleration and dissipating the seismic energy through damping (Chaudhary, Ab *et al.* 2001; Kim, Yi *et al.* 2008), but cannot reduce the seismic response of the bridge pier. Therefore, the ductility-based seismic design is increasingly applied for the railway bridge pier with bending failure mode under earthquakes. The bridge pier with ductility seismic design cannot avoid damage during earthquakes, which result in residual

deformations in the plastic region of the bridge pier after earthquakes. The repair and rebuilt of the damaged bridge piers not just influence the normal operation of transport system, but also are costly and time-consuming. The seismic isolation method for other structures with self-centering capacity (Li, Li *et al.* 2018) provide an optional way to prevent severe damage of bridge pier with large size during earthquakes. The rocking isolation system is designed by the separation of the bridge pier with the basement. Thus, rocking of the bridge pier may develop large nonlinear deformations when subjected to strong earthquakes but experience far less damage (Antonellis and Panagiotou 2014). Therefore, the seismic isolation design method is superior to the ductility-based seismic design method because it can reduce the strengthening or repairing cost after earthquakes (Saiidi and Maragakis 1999).

The research and application of the seismic isolation in bridge structures are being focused in recent decades. The first bridge designed and built with a rocking mechanism for seismic isolation is the South Rangitikei Rail Bridge of New Zealand completed in 1981 (Chen, Liao *et al.* 2006). The design concept of the Rion Antirion Bridge in Greek is also somehow similar to a base isolation system with a limitation of the forces transmitted to the superstructure whenever sliding occurs (Pecker 2004). The use of superelastic shape memory alloy (SMA) bars (Roh and Reinhorn 2010), post-tensioned steel stands (Marriott, Pampanin *et al.* 2009; Ming-Hua, Xin *et al.* 2012) in self-centering bridge pier with different joints between the pier and basement to control the rocking of the bridge piers. Leitner and Hao (2016) investigated various options (mild steel and superelastic shape memory alloy) for the improvement of energy dissipation capabilities of rocking

\*Corresponding author, Professor  
E-mail: [xiaxiushen@mail.lzjtu.cn](mailto:xiaxiushen@mail.lzjtu.cn)

bridge pier systems. The foundation type is also important for the rocking mechanism of the bridge pier. Mergos and Kawashima (2005) presented an analysis of a standard bridge supported by direct foundations and shows an isolation effect of inelastic rocking of the spread foundations. Anastasopoulos, Loli *et al.* (2013) found that the rocking-isolated bridge pier on surface foundation is effectively protected, surviving all seismic excitations without structural damage, at the cost of increased foundation settlement. Although a conventionally designed reinforced concrete (RC) pier on an adequately large shallow foundation would suffer structural failure of the RC column and collapse in an earthquake sufficiently exceeding its design limits, rocking motion of an alternative under designed foundation would allow the same pier to survive even extreme shaking scenarios (Loli, Knappett *et al.* 2014). While uplifting systems experience excessive displacements, in comparison with systems that are not allowed to uplift, ductility demand in the superstructure generally decreases owing to foundation uplift (Ghannad and Jafarieh 2014). Therefore, the displacement controlling of uplifting is essential for the isolated bridge pier with rocking vibration.

In this study, a seismic rocking-isolated system is presented and make it suitable for the railway bridge piers with large solid and hollow section. Besides, unbonded prestressed tendons are used to control the uplifting displacement of the rocking-isolated bridge pier. A numerical model of seismic isolation for the rocking bridge pier is presented, and validated by shaking table test of a scaled model bridge. In order to evaluate the seismic performance of the rocking-isolated bridge pier. Eventually, a seismic design procedure of the new isolation bridge pier is provided and applied by using a case study.

## 2. Designing of rocking-isolated bridge pier

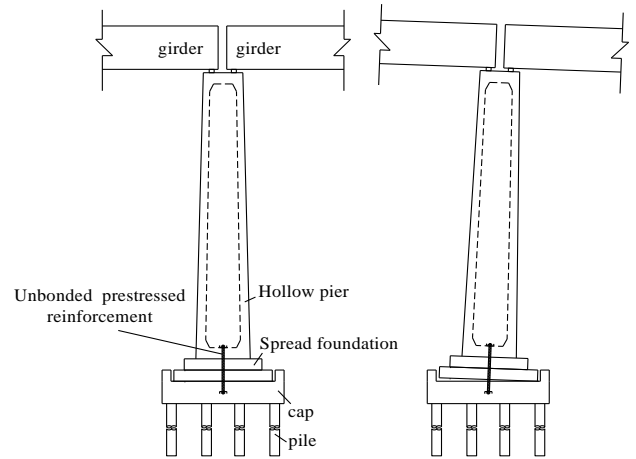
For the concrete railway bridge piers in China, the solid section with low longitudinal steel ratio is adopted when the pier height is less than 20m, and if the pier height is larger than 30m, the hollow section is preferred. The seismic rocking-isolated bridge pier used in this study is a self-centering system under small and moderate earthquakes. The large section size of the railway bridge pier made it easy to apply the unbonded prestressed tendons to prevent overturning under strong earthquakes. The structure details of the rocking-isolated bridge piers with hollow and solid section are shown in Figs.1 and 2.

The rocking seismic isolation mechanism can be concluded as follows.

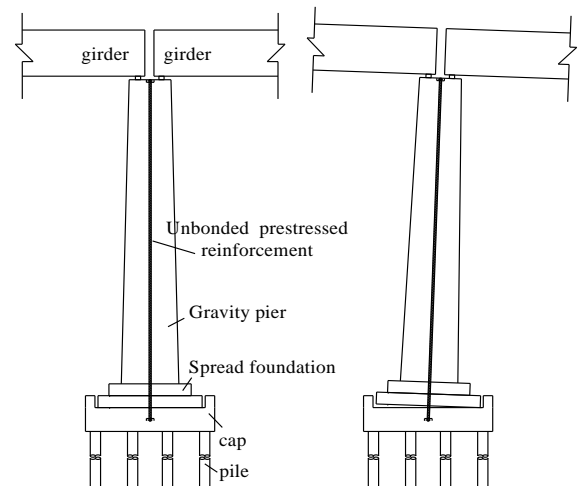
(1) The existing of the unbonded prestressed tendons increases vertical tensile stiffness between the pier and basement. The prestress raises the uplifting moment of the bridge pier and influences the rocking response;

(2) Tension force occurs in unbonded prestressed tendons after pier uplifting;

(3) The unbonded prestressed tendons will yield under strong or rare earthquakes.



(a) Rocking without uplifting (b) Rocking with uplifting  
Fig. 1 Structure detail of a rocking-isolated bridge pier with hollow section



(a) Rocking without uplifting (b) rocking with uplifting  
Fig. 2 Structure detail of a rocking-isolated bridge pier with solid section

## 3. Numerical model of the rocking-isolated bridge pier

Through pseudo-static test results, we presented a numerical model of the rocking-isolated bridge pier (two spring model), as shown in Fig. 3. The elastic beam element is used to simulate the bridge pier, basement and the spread foundation, the compression spring element without tension is used to simulate the uplifting of the bridge pier. While the prestressed tendon is simulated by tension spring element without compression, the force-displacement relationship is in accordance with the bi-linear model, as show in Fig. 4.

The numerical analysis is conducted with the assistance of the Opensees platform. The hysteretic relationship of the prestressed tendon is simulated with the uniaxial Material (ElasticPP) in Opensees, as shown in Fig. 5.

The  $\varepsilon_0$  in Fig.5 can be calculated by the Eq. (1):

$$\varepsilon_0 = -\frac{F_a}{EA} \quad (1)$$

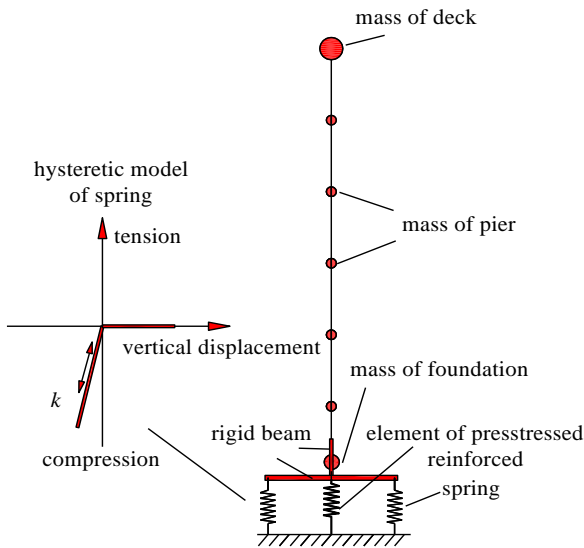


Fig. 3 Two spring model with prestressed tendon

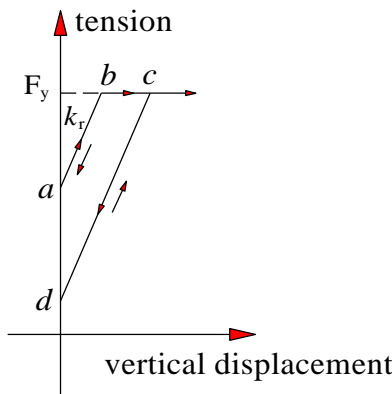


Fig. 4 Bi-linear model of the prestressed tendon

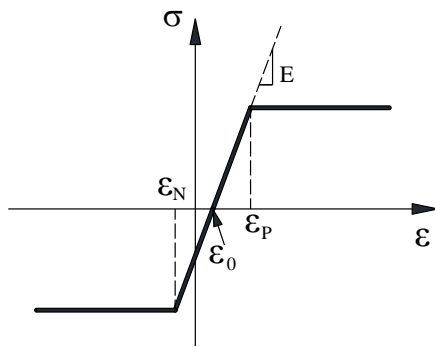


Fig. 5 ElasticPP constitutive relations

Where  $k$  is the compressive stiffness of the uplifted spring,  $k_r$  is the initial stiffness of the prestressed tendon,  $F_a$  and  $F_y$  are the initial tension and yield force of the prestressed tendon,  $\epsilon_P$  and  $\epsilon_N$  are the yield strains by tension and compression,  $\epsilon_0$  is the initial strain.

The force-displacement hysteretic curves of the top-pier are obtained by the above numerical method and compared with the results by pseudo-static tests, as shown in Figs. 6 and 7. Fig. 6 shows the hysteretic curves of the free rocking bridge pier without displacement constraint measures, and Fig. 7 shows the results of the controlled rocking bridge

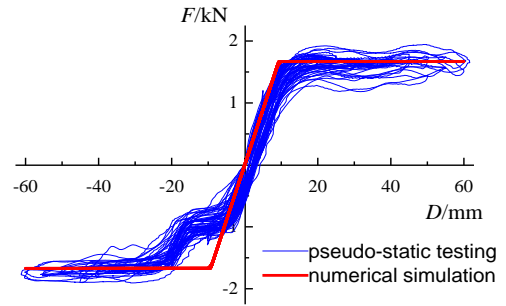


Fig. 6 Hysteretic curves of free rocking-isolated pier

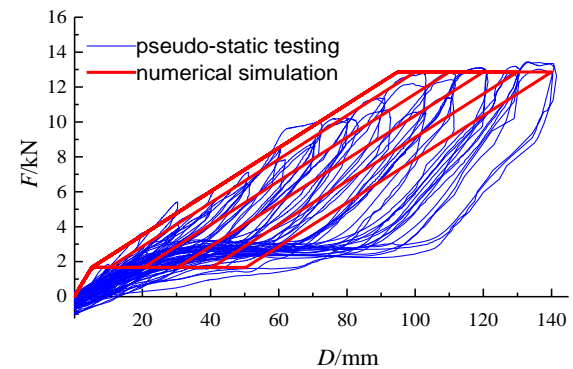


Fig. 7 Hysteretic curves of controlled rocking-isolated pier

pier with prestressed tendon. These satisfied calculated results validated the numerical model for the free and controlled rocking bridge pier.

#### 4. Shaking table test of the rocking-isolated bridge pier

##### 4.1 Model design

The size of the earthquake shaking table used in this study is 4m×4m. The test model consists of three main parts, i.e. the steel beam with H-type, the bridge pier and the basement. The H-type steel beam simulate the superstructure of the bridge, weighs 663kg. One of the bridge piers is fixed and the other is the seismic rocking bridge pier with self-centering function. The measured compression strength of the concrete with a cube specimen (150mm×150mm×150mm) is 32.58MPa, and the measured elasticity modulus with a prismatic specimen (150mm×150mm×300mm) is 32200MPa. The hot-rolled deformed steel bar with a diameter of 12mm is used as the prestressed tendon in the rocking bridge pier, its elasticity modulus, yield strength and tension strength are 192GPa, 312MPa and 486MPa. The arrangement of the shaking table test is shown in Fig. 8.

##### 4.2 Testing method

The self-centering bridge pier and the detailed arrangement of the measuring points are shown in Fig. 9. The acceleration sensors (A1-A18), displacement sensors (D1-D4) and electric resistance strain gage are used during the shaking table test.



Fig. 8 Arrangement of the shaking table test

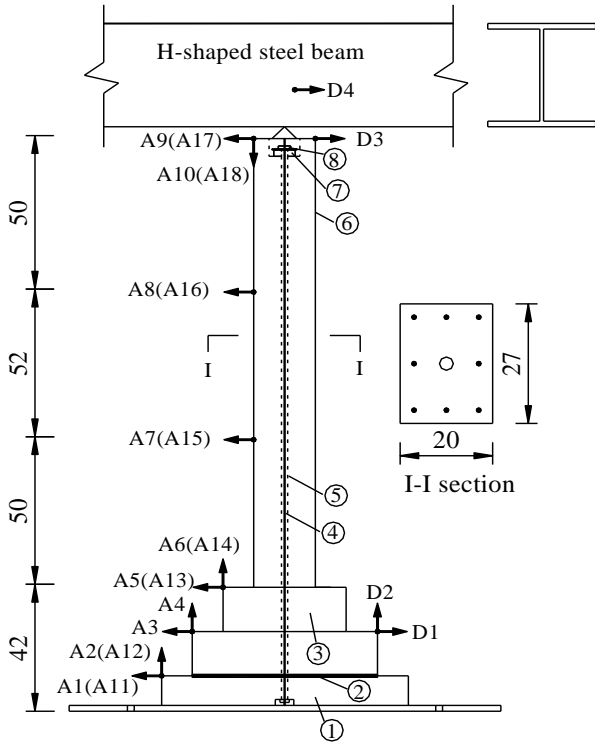


Fig. 9 Self-centering bridge pier and the arrangement of measuring points (unit: cm): ①-basement, ②-uplifting surface, ③-expanded bridge pier, ④-unbonded prestressed tendon, ⑤-reserved pore canal, ⑥-self-centering bridge pier, ⑦-pressure sensor, ⑧-anchor device for prestress

The EI-Centro seismic record in 1940, the Mexico seismic records in 1985 and the Chi-Chi seismic record in 1999 are selected as the input by adjusting the peak ground acceleration (PGA). The fundamental frequency (FF), damping ratio (DR) and the seismic response are listed in Table 1.

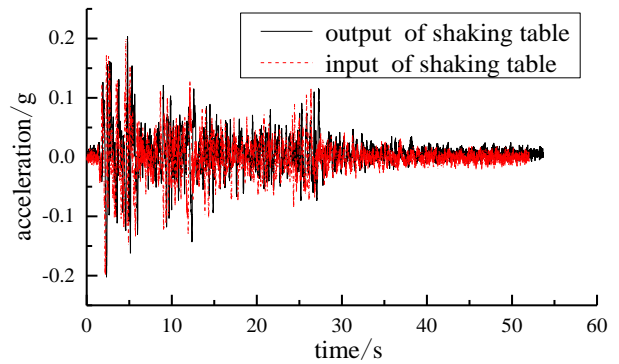


Fig. 10 Input and output of the EI-Centro seismic record

### 4.3 Table shaking test results and analysis

The output of seismic records (EI-Centro waves) from the shaking table is agree well with the input records, as shown in Fig. 10. The uplift at the pier footing occurs at the peak ground acceleration (PGA) of 0.15g, no obvious rocking appears in the isolated pier. When the PGA reaches to 0.20g, uplift displacement at pier footing and lateral displacement at pier top increase, large rocking appears in isolated pier and the superstructure start to swing, no obvious visible cracks exist at the pier after shaking. The base frequency of the pier is obtained of 5.75Hz by white noise sweeping, and the damping ratio is 8.9%.

The lateral displacement and acceleration time histories at pier-top, bending moment at pier-footing histories are shown in Figs. 11-13. From Figs. 11-13, it can be found that the numerical simulation results are accordant with the shaking table testing results. Besides, abnormal values (cuspidal points) occur in time-history curves of the displacement, acceleration and bending moment (about 12s). The main reason is that there exists collision between the rocking pier and the basement surface during pier uplifting.

Table 1 Test condition and the top-pier lateral response

Test condition	Seismic records	PGA/g		FF/Hz	DR/%	Top-pier lateral response	
		input	output			displacement/mm	acceleration/(m.s <sup>-2</sup> )
1	First white noise	0.07	0.35	5.75	8.9	0.96	25.11
2	El-Centro	0.15	0.15	--	--	9.01	4.02
3	Mexico	0.15	0.11	--	--	16.87	2.45
4	Chi-Chi	0.15	0.14	--	--	9.81	4.37
5	Second white noise	0.07	0.18	5.25	9.1	0.68	4.67
6	El-Centro	0.20	0.20	--	--	14.31	6.58
7	Mexico	0.20	0.18	--	--	19.26	6.92
8	Chi-Chi	0.20	0.19	--	--	12.18	17.64
9	Third white noise	0.07	0.23	4.56	9.3	0.61	6.08

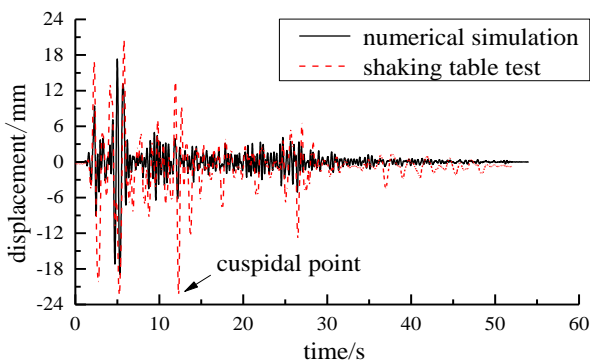


Fig. 11 Numerical and experimental values of the top-pier displacement

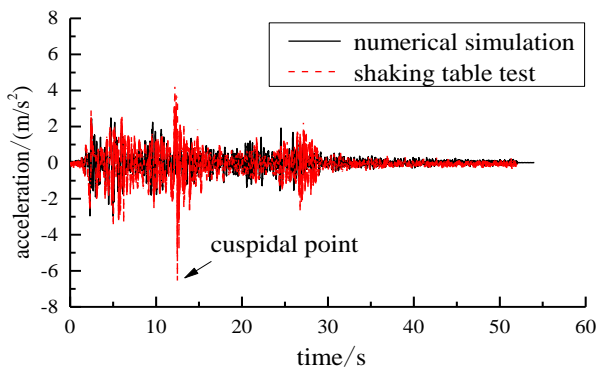


Fig. 12 Numerical and experimental values of the top-pier acceleration

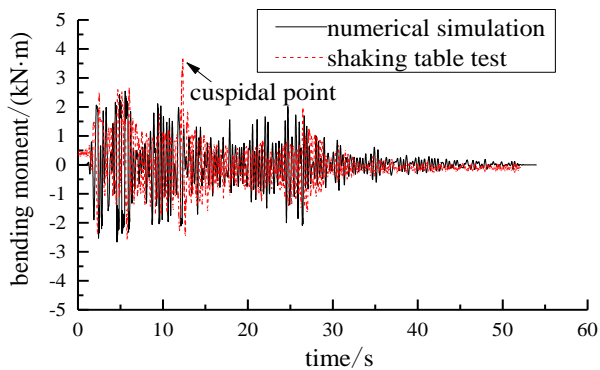


Fig. 13 Numerical and experimental values of the bottom-pier bending moment

## 5. Seismic design method of the rocking-isolated bridge pier

### 5.1 Design method and procedure

A design method and its detailed procedure of the rocking-isolated bridge pier are presented in this study, as shown in Fig. 14.

### 5.2 Design example

Based on the presented design method, a design example is carried out. A simply-supported beam bridge with 32-m span for single-track line railway is selected, it has hollow piers with round end rectangular section and pile group foundation, as shown in Fig. 15.

The end round diameter of the original hollow pier is 7m, the straight line between the two semi-circle is 2.1m, and the size of rectangular bearing platform is 1.27m × 1.45m, as shown in Fig. 16 (a). The original design scheme is changed to improve the seismic performance of the bridge, and the rocking-isolated bridge pier is adopted in the new design scheme. A spread foundation is added at the bottom of the original pier, its size is 10m × 12m × 2m, 2m height of concrete blocks are added at the bearing platform to limit the pier slide after uplifting, as shown in Fig. 16 (b). Four unbonded prestressed tendons with a diameter of 32mm are installed through the section center of hollow pier to the bearing platform, which can provide initial lateral stiffness of the bridge pier-pile foundation system under normal condition and frequent earthquake. When the severe earthquake occurs, overturning can be avoided due to restraining of the prestressed tendons even under large uplifting and lateral sliding.

#### (1) Seismic design for frequent earthquakes

The seismic design method of the new isolated bridge pier has no difference with the original one under frequent earthquakes without uplifting of the upper part. For frequent earthquake in areas of basic seismic intensity of VII ( $a_g=0.1g$ ), seismic forces including bending moment and shear force are calculated by the response spectrum analysis method, i.e.  $M=99370$  kN.m,  $Q=2260$  kN. It is assumed that there is no prestressing loss under frequent earthquakes,

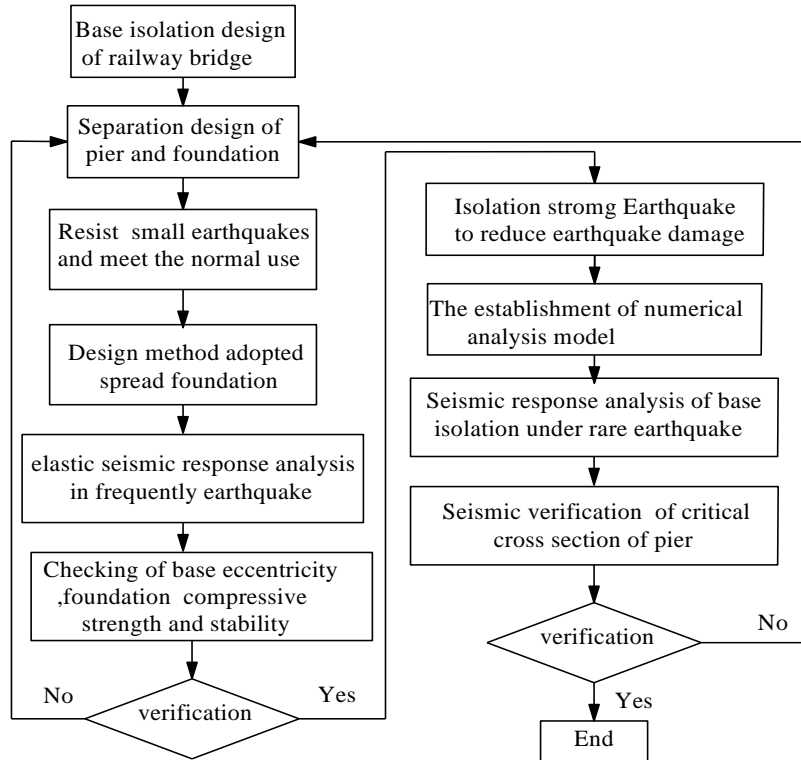


Fig. 14 Design procedure of the rocking-isolated bridge pier

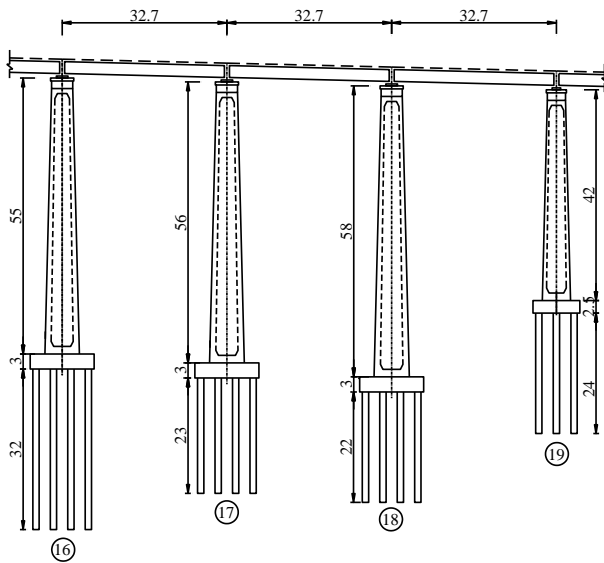


Fig. 15 Configuration of a typical tall pier railway bridge (unit: m)

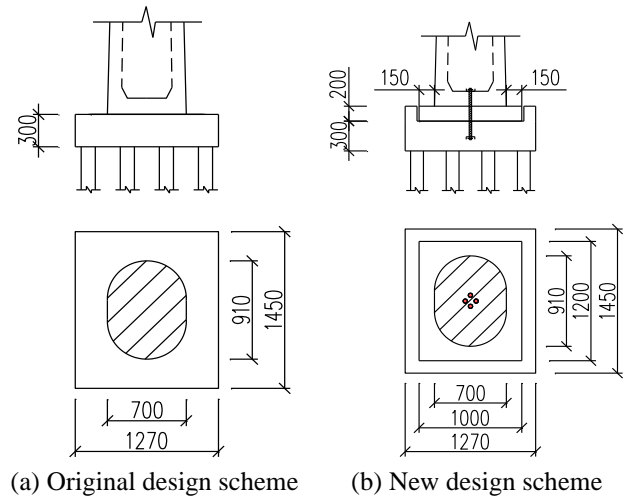


Fig. 16 Design scheme of bridge pier (unit: cm)

thus the vertical axial load at the bottom of the spread foundation is calculated as  $N=42111\text{kN}$ . Based on the Code for seismic design of railway engineering, the decentration of the composite force and compression strength at the basement, and the stability are used to evaluate the seismic performance, as listed in Table 2. From Table 2, it can be found that the new isolated bridge pier can satisfy the seismic requirement of Chinese code. The results show that the bridge pier is still in the range of elasticity and no uplift and slide occur under frequent earthquakes. If the seismic requirement is not satisfied, the isolated bridge pier will be

redesigned by increasing the prestressing force of the unbonded tendons or enlarging the size of the added spread foundation.

(2) Seismic design for rare earthquakes

The seismic records of EI-centro in 1940, Northridge in 1994 and Taft in 1952 from PEER database are selected as the input ground motion, as listed in Table 3. PGA, PGV and PGD in Table 3 are the peak ground acceleration, peak ground velocity and peak ground displacement, respectively. Key parameters of the prestressed tendon in Figs. 4 and 5 should be  $k=2.1 \times 10^8 \text{ kN/m}$ ,  $F_a=4512 \text{ kN}$ , and  $F_y=5394 \text{ kN}$ , from Eq.(1), it can be calculated as  $\epsilon_0=-0.0072$ . Based on the Caltrans seismic design criteria,  $\epsilon_p=0.0086$ .

Table 2 Verification of seismic performance under frequent earthquake

Decentration distance /m		Compression strength /MPa		Anti-slide force /kN		Anti-overturning moment /kN.m	
$e$	$[e]$	$\sigma_{\max}$	$[\sigma]$	$1.1Q$	$[Q]$	$1.3M$	$[M]$
2.4	5.8	0.8	15	2486	25267	129181	210555

Table 3 Parameters of the seismic records

Seismic records	Earthquake magnitude	PGA/g	PGV/ (cm.s <sup>-1</sup> )	PGD/cm
1940 El-centro	7.0	0.313	29.8	13.32
1994 Northridge	6.7	0.516	62.8	11.08
1952 Taft	7.4	0.178	17.5	8.99

Table 4 Seismic response of the bridge pier

Seismic records	Pier-top displacement /cm	Pier-bottom bending moment /kN.m	Uplifting displacement / mm	Tension of the prestressed tendon /kN
1940 El-centro	25.8	260980	15.6	5394
1952 Taft	16.2	245095	7.5	5394
1994 Northridge	36.3	326499	25.4	5394

The acceleration amplitude of the three seismic records is 0.57g under rare earthquakes. The pier-top displacement and pier-bottom bending moment are calculated, as listed in Table 4. Moreover, uplift occurs and the prestressed tendons yield under rare earthquakes, the uplifting displacement and tension of the prestressed tendon are calculated, as listed in Table 4.

The tension developing of the prestressed tendon over time is shown in Fig.17. The prestress loss and yielding of the unbonded tendons are beneficial for the seismic isolation of the new bridge pier. The maximum uplifting displacement is about 2.54cm, which is acceptable in seismic design under rare earthquakes.

## 6. Conclusions

Seismic isolation bridge piers with rocking method based on a self-centering system are presented in this study. Numerical simulation and shaking table test of the new designed bridge piers are conducted, and some conclusions are drawn as follows.

- The seismic isolation bridge pier used in this study is a self-centering system by rocking method under small and moderate earthquakes. The large section size of the railway bridge pier makes it easy to apply the unbonded prestressed tendons to prevent overturning under strong earthquakes.

- Through pseudo-static test results, a numerical model of the isolated bridge pier (two spring model) is presented. The compression spring element without tension is used to simulate the uplifting of the bridge pier, while the

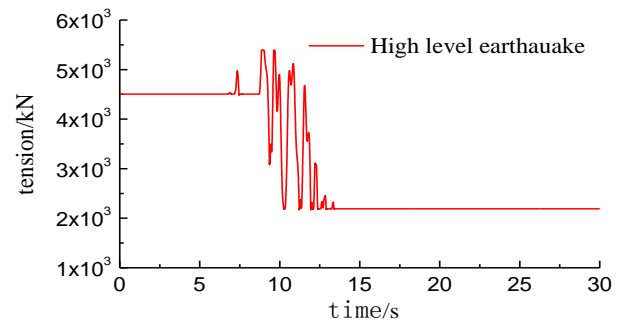


Fig. 17 Tension of prestressed tendon over time

prestressed tendon is simulated by tension spring element without compression.

- Shaking table test is carried out to validate the numerical model (two spring model) and further evaluate the seismic performance of the isolated bridge piers. It is found that the uplift at the pier footing occurs at the peak ground acceleration (PGA) of 0.15g, when the PGA reaches to 0.20g, large rocking appears in the bridge pier with the increasing uplifting displacement at pier footing and the lateral displacement at pier top, and no obvious visible cracks exist at the pier after shaking.

- The detailed procedures for seismic design of the isolated bridge pier with rocking method are presented and a case study is carried out based on the provided method. It is shown that the prestress loss and yielding of the unbonded tendons are beneficial for the seismic isolation of the new bridge pier. The maximum uplifting displacement is acceptable in seismic design under rare earthquakes.

## Acknowledgement

This research is supported by the National Natural Science Foundation of China (Grant No. 51368033, 51768036, and 51668035), National Natural Science Foundation of China for Young Scholar (Grant No. 51808273), Technology research and development Project of China Railways Corporation (2015G002-B), Project funded by China Postdoctoral Science Foundation (Xiyin Zhang), Tianyou Youth Talent Lift Program of Lanzhou Jiaotong University (Xiyin Zhang) and lzjtu (201801) EP support. On behalf of all authors, the corresponding author states that there is no conflict of interest.

## References

- Anastasopoulos, I., Loli, M., Georgarakos, T. and Drosos, V. (2013), "Shaking Table Testing of Rocking—Isolated Bridge Pier on Sand", *J. Earthq. Eng.*, **17**(1), 1-32. <https://doi.org/10.1080/13632469.2012.705225>.
- Antonellis, G. and Panagiotou, M. (2014), "Seismic Response of Bridges with Rocking Foundations Compared to Fixed-Base Bridges at a Near-Fault Site", *J. Bridge Eng.*, **19**(5), 04014007. [https://doi.org/10.1061/\(ASCE\)BE.1943-5592.0000570](https://doi.org/10.1061/(ASCE)BE.1943-5592.0000570).
- Chaudhary, M.T.A., Ab, Eacute, M. and Fujino, Y. (2001), "Performance evaluation of base-isolated Yama-agé bridge with high damping rubber bearings using recorded seismic data", *Eng. Struct.*, **23**(8), 902-910. <https://doi.org/10.1016/S0141->

- 0296(00)00117-6.
- Chen, X., Ding, M., Zhang, X., Liu, Z. and Ma, H. (2018), "Experimental investigation on seismic retrofit of gravity railway bridge pier with CFRP and steel materials", *Construct. Build. Mater.*, **182**, 371-384. <https://doi.org/10.1016/j.conbuildmat.2018.06.102>.
- Chen, Y.-H., Liao, W.-H., Lee, C.-L. and Wang, Y.-P. (2006), "Seismic isolation of viaduct piers by means of a rocking mechanism", *Earthq. Eng. Struct. Dynam.*, **35**(6), 713-736. <https://doi.org/10.1002/eqe.555>.
- Chen, Z., Han, Z., Fang, H. and Wei, K. (2018), "Seismic vibration control for bridges with high-piers in Sichuan-Tibet Railway", *Struct. Eng. Mech.*, **66**(6), 749-759. <https://doi.org/10.12989/sem.2018.66.6.749>.
- Chung, Y.S., Park, C.K. and Lee, D.H. (2006), "Seismic performance of RC bridge piers subjected to moderate earthquakes", *Struct. Eng. Mech.*, **24**(4), 429-446. <https://doi.org/10.12989/sem.2006.24.4.429>.
- Ding, M., Chen, X., Zhang, X., Liu, Z. and Lu, J. (2018), "Study on seismic strengthening of railway bridge pier with CFRP and concrete jackets", *Earthq. Struct.*, **15**(3), 275-283. <https://doi.org/10.12989/eas.2018.15.3.275>.
- Fragiadakis, M., Vamvatsikos, D., Karlaftis, M.G., Lagaros, N.D. and Papadrakakis, M. (2015), "Seismic assessment of structures and lifelines", *J. Sound Vib.*, **334**, 29-56. <https://doi.org/10.1016/j.jsv.2013.12.031>.
- Ghannad, M.A. and Jafarieh, A.H. (2014), "Inelastic displacement ratios for soil-structure systems allowed to uplift", *Earthq. Eng. Struct. Dynam.*, **43**(9), 1401-1421. <https://doi.org/10.1002/eqe.2405>.
- Heo, G., Kim, C., Jeon, S., Lee, C. and Jeon, J. (2017), "A hybrid seismic response control to improve performance of a two-span bridge", *Struct. Eng. Mech.*, **61**(5), 675-684. <https://doi.org/10.12989/sem.2017.61.5.675>.
- Kim, D., Yi, J.-H., Seo, H.-Y. and Chang, C. (2008), "Earthquake risk assessment of seismically isolated extradosed bridges with lead rubber bearings", *Struct. Eng. Mech.*, **29**(6), 689-708. <https://doi.org/10.12989/sem.2008.29.6.689>.
- Leitner, E.J. and Hao, H. (2016), "Three-dimensional finite element modelling of rocking bridge piers under cyclic loading and exploration of options for increased energy dissipation", *Eng. Struct.*, **118**, 74-88. <https://doi.org/10.1016/j.engstruct.2016.03.042>.
- Li, J., Guan, Z. and Liang, Z. (2014), "Rational analysis model and seismic behaviour of tall bridge piers", *Struct. Eng. Mech.*, **51**(1), 131-140. <https://doi.org/10.12989/sem.2014.51.1.131>.
- Li, L.X., Li, H.N. and Li, C. (2018), "Seismic fragility assessment of self-centering RC frame structures considering maximum and residual deformations", *Struct. Eng. Mech.*, **68**(6), 677-689. <https://doi.org/10.12989/sem.2018.68.6.677>.
- Loli, M., Knappett, J.A., Brown, M.J., Anastasopoulos, I. and Gazetas, G. (2014), "Centrifuge modeling of rocking-isolated inelastic RC bridge piers", *Earthq. Eng. Struct. Dynam.*, **43**(15), 2341-2359. <https://doi.org/10.1002/eqe.2451>.
- Marriott, D., Pampanin, S. and Palermo, A. (2009), "Quasi-static and pseudo-dynamic testing of unbonded post-tensioned rocking bridge piers with external replaceable dissipaters", *Earthq. Eng. Struct. Dynam.*, **38**(3), 331-354. <https://doi.org/10.1002/eqe.857>.
- Mergos, P.E. and Kawashima, K. (2005), "Rocking isolation of a typical bridge pier on spread foundation", *J. Earthq. Eng.*, **9**(sup2), 395-414. <https://doi.org/10.1142/S1363246905002456>.
- Ming-Hua, H.E., Xin, K.G. and Guo, J. (2012), "Local stability study of new bridge piers with self-centering joints", *Eng. Mech.*, **29**(4), 122-127.
- Ozdemir, G., Bayhan, B. and Gulkan, P. (2018), "Variations in the hysteretic behavior of LRBs as a function of applied loading", *Struct. Eng. Mech.*, **67**(1), 69-78. <https://doi.org/10.12989/sem.2018.67.1.069>.
- Pecker, A. (2004). "Design and Construction of the Rion Antirion Bridge", *Geotrans 2004*, Los Angeles, California, U.S.A., July.
- Roh, H. and Reinhorn, A.M. (2010), "Hysteretic behavior of precast segmental bridge piers with superelastic shape memory alloy bars", *Eng. Struct.*, **32**(10), 3394-3403. <https://doi.org/10.1016/j.engstruct.2010.07.013>.
- Saïidi, M. and Maragakis, E. (1999), "Effect of base isolation on the seismic response of multi-column bridges", *Struct. Eng. Mech.*, **8**(4), 411-419. <https://doi.org/10.12989/sem.1999.8.4.411>.
- Shao, C., Ju, J.-w.W., Han, G. and Qian, Y. (2017), "Seismic applicability of a long-span railway concrete upper-deck arch bridge with CFST rigid skeleton rib", *Struct. Eng. Mech.*, **61**(5), 645-655. <https://doi.org/10.12989/sem.2017.61.5.645>.

CC